Phonon transport across a vacuum gap

D. P. Sellan, E. S. Landry, K. Sasihithlu, A. Narayanaswamy, A. J. H. McGaughey, and C. H. Amon

Phys. Rev. B **85**, 024118 — Published 23 January 2012

DOI: 10.1103/PhysRevB.85.024118

Phonon transport across a vacuum gap

D. P. Sellan,[1] E. S. Landry,[2,3] K. Sasihithlu,[4] A. Narayanaswamy,[4] A. J. H. McGaughey*,[3] and C. H. Amon[1,3]

[1]*Department of Mechanical & Industrial Engineering, University of Toronto, Toronto, Ontario M5S 3G8, Canada*
[2]*United Technologies Research Center, East Hartford, Connecticut 06108, USA*
[3]*Department of Mechanical Engineering, Carnegie Mellon University, Pittsburgh, Pennsylvania 15213, USA*
[4]*Department of Mechanical Engineering, Columbia University, New York, New York 10027, USA*

(Dated: January 9, 2012)

Phonon transport across a silicon/vacuum-gap/silicon structure is modeled using lattice dynamics calculations and Landauer theory. The phonons transmit thermal energy across the vacuum gap via atomic interactions between the leads. Because the incident phonons do not encounter a classically impenetrable potential barrier, this mechanism is not a tunneling phenomenon. While some incident phonons transmit across the vacuum-gap and remain in their original mode, many are annihilated and excite different modes. We show that the heat flux due to phonon transport can be four orders of magnitude larger than that due to photon transport predicted from near-field radiation theory.

PACS numbers: 44.10.+i, 63.22.Np, 68.35.Ja, 68.37.Ef

I. INTRODUCTION

Although phonons require matter to exist and cannot propagate in bulk vacuum, recent experimental[1] and theoretical[2,3] reports have shown that phonons can transport across vacuum-gaps a few angstroms wide. Vacuum phonon transport is a parallel heat-transfer process to near-field radiation, although the length scales over which the two phenomena dominate are different. Accounting for it is important in atomic force microscopy (AFM) and scanning tunneling microscopy (STM) measurements, where an angstrom-sized gap is present between the microscope tip and the sample. Studying phonon transport across small gaps is also relevant to predicting the thermal resistance of rough interfaces[4,5] and in accounting for thermal resistance due to the presence of nanovoids.[6]

Using ultrahigh-vacuum inelastic STM, Altfeder et al.[1] studied the thermal coupling between a Pt/Ir STM-tip and a Au(111) film separated by 3 $\AA$ of vacuum. They found that the local electric field of the STM tip couples the thermal vibrations of the tip and the film. The resulting heat flux was six orders of magnitude larger than predictions of near-field radiation theory. Using piezoelectric leads, Prunnila and Meltaus[2] theoretically showed that thermal energy can transport across a vacuum-gap via an electric field induced by acoustic phonons. Making the Debye approximation for the material properties (i.e., isotropic and linear dispersion, no optical phonons), they report the angle-of-incidence- and wave vector magnitude-dependence of the phonon transmission coefficients and the vacuum thermal conductance for a ZnO/vacuum-gap/ZnO system. No information is provided about what phonon modes are excited on the other side of the gap. Mahan[3] also showed that phonons can transport across vacuum-gaps up to a few nanometers wide as a result of polar effects. The mechanism described by Prunnila and Meltaus[2] and Mahan[3] does not exist in non-polar materials (e.g., silicon), where the lattice strain induced by phonons does not induce a macroscopic electric field.

In this work, we use lattice dynamics calculations to show that phonons can transport across a vacuum gap via atomic interactions between the leads. This mechanism will exist in all materials. Because phonons cannot propagate in bulk vacuum, it may seem reasonable to call vacuum phonon transport a tunneling phenomenon. The mechanism we identify, however, is not a tunneling phenomenon because the phonons that transmit across the vacuum-gap do not encounter a classically impenetrable potential barrier. Instead, phonons classically transmit through channels of allowed vibrational states that only exist for small enough vacuum-gap widths.

This mechanism is supported by lattice dynamics modeling work by Landry and McGaughey[7] on germanium thin films bounded by silicon. They report that phonons with frequencies that are not permitted in bulk germanium can pass through germanium films thinner than 2 nm. Tian et al.[8] reported similar results for mass-mismatched Lennard-Jones thin film systems using the classical molecular dynamics-based phonon wave-packet technique. Landry and McGaughey explained their result by showing that the density of states of sub-2 nm germanium thin films are not bulk-like and take on vibrational qualities of silicon. Specifically, the maximum permitted frequency in the film ($\omega^{max}_{\mathrm{Ge}-film}$) is greater than the maximum permitted frequency in the bulk ($\omega^{max}_{\mathrm{Ge}-bulk}$). Phonons that pass through

* Corresponding author: mcgaughey@cmu.edu

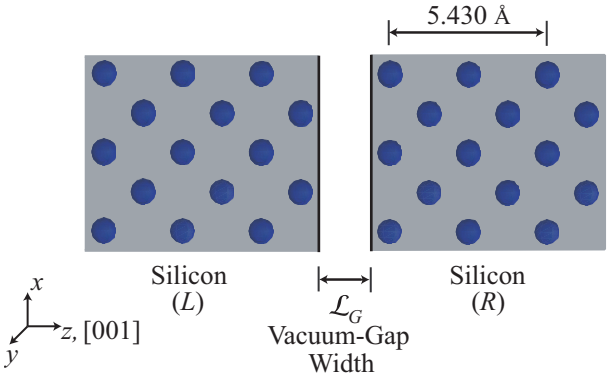

FIG. 1: (color online) Schematic diagram of the three-dimensional Si/vacuum-gap/Si structure for $\mathcal{L}_G = 1.72$ Å. The shaded region between the dark silicon atoms is the volume associated with the perfect silicon crystal. Vacuum space, shown in white, is added to form the vacuum-gap. What we call vacuum space is in fact a region of finite electron density. The structure is periodic in the x and y directions and semi-infinite in the negative and positive z directions.

the germanium thin film with frequencies between $\omega^{max}_{\text{Ge}-bulk}$ and $\omega^{max}_{\text{Ge}-film}$ thus do not tunnel but are classically transmitted because the phonon density of states of the film permits them to exist. In other words, the transmitted phonons never encounter a classically impenetrable potential barrier.

Using a similar approach to that of Landry and McGaughey, we herein examine phonon transport through a Si/vacuum-gap/Si structure, which is described in Sec. II. We first use lattice dynamics calculations to predict mode-dependent phonon transport properties (frequencies, group velocities, and transmission coefficients) in Secs. II and III. These phonon properties and Landauer theory are then used in Sec. IV to predict the vacuum-gap thermal resistance. We compare these resistances to phonon resistances of a Si/Si grain boundary and a Si/Ge interface as well as the resistance to photon energy transport for a Si/vacuum-gap/Si structure predicted by near-field radiation theory.

II. VACUUM-GAP STRUCTURE

To build the Si/vacuum-gap/Si structures, we begin with a perfect silicon crystal with a lattice constant of 5.430 Å (Ref. 9). Vacuum space is added between two atomic layers to form the vacuum-gap, as shown in Fig. 1. Note that $\mathcal{L}_G$, the vacuum-gap width, is defined as the z component of vacuum space, shown in white, and is the distance added to the perfect silicon structure. For small enough vacuum-gap widths, the vacuum-gap is in fact a region of finite electron density that results in atomic interactions between the leads. Using the Stillinger-Weber potential to describe the atomic interactions,[10] we perform harmonic lattice dynamics calculations to predict bulk phonon frequencies, $\omega(\boldsymbol{\kappa}, \nu)$ and group velocity vectors, $\mathbf{v}_g(\boldsymbol{\kappa}, \nu)$,[11,12] for 10000 randomly sampled phonon modes in the first Brillouin zone. Each phonon mode is identified by its wave vector, $\boldsymbol{\kappa}$, and dispersion branch, ν. We find that evaluating 10000 modes is sufficient to provide converged values of the phonon resistances predicted in Sec. IV.

III. PHONON TRANSMISSION COEFFICIENTS

With the bulk phonon properties we next predict mode-dependent phonon transmission coefficients, $\alpha_{L\rightarrow R}(\boldsymbol{\kappa}, \nu, \mathcal{L}_G)$, defined as the fraction of incident phonon energy that is transmitted from the left silicon lead (L) to the right silicon lead (R) [similar for $\alpha_{R\rightarrow L}(\boldsymbol{\kappa}, \nu, \mathcal{L}_G)$, which is identical to $\alpha_{L\rightarrow R}(\boldsymbol{\kappa}, \nu, \mathcal{L}_G)$ for our symmetrical structure]. Phonon transmission coefficients are often calculated using the acoustic mismatch model (AMM) or the diffuse mismatch model (DMM).[4] Our Si/vacuum-gap/Si structures have the same bulk material on either side of the vacuum-gap. Since both the AMM and DMM rely only on bulk phonon properties and do not include details of the atomic structure at the interface, they cannot be used to describe phonon transport across the vacuum-gap. Instead, we use the scattering boundary method,[7,13–15] which considers the atomic-level detail.

The scattering boundary method is based on harmonic lattice dynamics theory and assumes that phonon scattering at the Si/vacuum-gap boundaries is elastic and specular. The assumption of elastic scattering [i.e., the reflected and transmitted phonons have the same frequency as the incident phonon and $\alpha_{L\rightarrow R}(\boldsymbol{\kappa}, \nu, \mathcal{L}_G)$ is temperature independent] is valid at low temperatures. Landry and McGaughey[14] report that this condition is met for Stillinger-Weber Si/Ge

interface systems with temperatures less than $T = 500$ K. This temperature-independence of thermal boundary resistance at low temperatures is also observed experimentally.[16] The assumption of specular scattering is valid for the vacuum-gap structures investigated here because they contain no defects or roughness that would promote diffuse scattering. In a real system, however, reconstruction of the free silicon surfaces may occur, leading to a probability that incident phonons will scatter diffusely.

For the Si/vacuum-gap/Si structures, the atomic interactions between the leads are truncated at the Stillinger-Weber cutoff radius, which corresponds to an absolute atom-atom distance of 3.77 $\mathring{A}$ / vacuum-gap width of $\mathcal{L}_G^{cutoff} = 1.89$ $\mathring{A}$. For systems with $\mathcal{L}_G > 1.89$ $\mathring{A}$, there is no communication between the left and right leads [i.e., $\alpha_{L\rightarrow R}(\boldsymbol{\kappa}, \nu, \mathcal{L}_G) = 0$ for all phonon modes] and the vacuum-gap is a bulk vacuum where phonons cannot propagate. The gap is thus a classically impenetrable potential barrier. For structures with vacuum-gaps less than 1.89 $\mathring{A}$, however, the left and right leads exchange vibrational energy via atomic interactions. The smaller the gap, the stronger the interaction between the leads, and the more channels of allowed vibrational states that are available within the gap for incident phonons to transmit energy. This trend is illustrated in the mode-dependent phonon transmission coefficients presented in Fig. 2(a) for $\mathcal{L}_G = 0.02$ and 1.72 $\mathring{A}$. For the $\mathcal{L}_G = 0.02$ $\mathring{A}$ structure, the left and right leads strongly interact and many incident phonon modes transport all of their vibrational energy across the vacuum-gap [i.e., $\alpha_{L\rightarrow R}(\boldsymbol{\kappa}, \nu, \mathcal{L}_G) = 1$ for many phonon modes]. Because silicon is a non-polar material, the lattice strain induced by phonons does not induce a macroscopic electric field. The electric-field/lattice-deformation coupling mechanism proposed by Prunnila and Meltaus[2] is therefore not present. Thus, we find that even very small vacuum-gaps block some phonon transport. For $\mathcal{L}_G = 1.72$ $\mathring{A}$, the leads weakly interact and $\alpha_{L\rightarrow R}(\boldsymbol{\kappa}, \nu, \mathcal{L}_G) > 0$ for only a few low-frequency phonon modes. If materials with Coulombic interactions are investigated [e.g., oxides, DNA (Ref. 17)], communication via atomic interactions (in addition to electric-field/lattice-deformation coupling effects) can be expected for larger vacuum-gaps.

We find that the magnitude of $\alpha_{L\rightarrow R}(\boldsymbol{\kappa}, \nu, \mathcal{L}_G)$ generally depends on (i) the polarization and direction-of-travel of the incident phonon mode with respect to the vacuum-gap and (ii) the magnitude of $\kappa_z \mathcal{L}_G$, where κ_z is the z component of the wave vector. Prunilla and Meltaus[2] report similar dependencies for ZnO/vacuum-gap/ZnO structures. For the $\mathcal{L}_G = 1.72$ $\mathring{A}$ structure, $\alpha_{L\rightarrow R}(\boldsymbol{\kappa}, \nu, \mathcal{L}_G)$ is largest for acoustic modes that (i) are polarized orthogonal to their direction-of-travel (i.e., transverse modes) whose associated atomic motions extend into the vacuum-gap, and (ii) have $\kappa_z \mathcal{L}_G < 1$. For very small vacuum-gaps, $\kappa_z \mathcal{L}_G \ll 1$ for all phonon modes and $\alpha_{L\rightarrow R}(\boldsymbol{\kappa}, \nu, \mathcal{L}_G)$ depends strongly on the phonon angle-of-incidence and is branch-independent. The greater the angle between the incident phonon velocity vector and the normal of the Si/vacuum-gap boundary, the less likely that phonon mode is to transport its vibrational energy across the vacuum-gap. Landry and McGaughey[7] report a similar angle-of-incidence dependence for their Si/Ge/Si and Ge/Si/Ge structures.

The mode-dependent phonon transmission coefficients plotted in Fig. 2(a) describe the fraction of incident phonon energy that transmits across the vacuum-gap. They do not describe which phonon modes are excited in the right lead. In Fig. 2(b), the fraction, $\eta(\boldsymbol{\kappa}, \nu, \mathcal{L}_G)$, of transmitted energy that remains in its incident phonon mode as it crosses the vacuum-gap is plotted for modes with $\alpha_{L\rightarrow R}(\boldsymbol{\kappa}, \nu, \mathcal{L}_G) > 0.01$ for $\mathcal{L}_G = 0.02$ and 1.72 $\mathring{A}$. For a system with no vacuum-gap, all transmitted phonon energy remains in its original phonon mode as it crosses the junction [i.e., $\eta(\boldsymbol{\kappa}, \nu, \mathcal{L}_G) = 1$ for all phonon modes]. As $\mathcal{L}_G$ increases, some of the transmitted phonon energy excites different modes in the right lead as it crosses the vacuum-gap [i.e., $\eta(\boldsymbol{\kappa}, \nu, \mathcal{L}_G) < 1$ for some phonon modes]. For the $\mathcal{L}_G = 0.02$ $\mathring{A}$ structure, $\eta(\boldsymbol{\kappa}, \nu, \mathcal{L}_G)$ shows a strong correlation with the bulk phonon density of states in the right lead, which is plotted in Fig. 2(c). The greater the phonon density of states in the right lead, the more modes that are available to excite, and the less likely transmitted phonon energy is to remain in its original mode. For the $\mathcal{L}_G = 1.72$ $\mathring{A}$ structure, $\eta(\boldsymbol{\kappa}, \nu, \mathcal{L}_G) < 1$ for the majority of the transmitted phonon modes.

IV. VACUUM THERMAL RESISTANCE

The phonon thermal resistance of the vacuum-gap can be calculated using the mode-dependent phonon transmission coefficients. The most commonly-applied expression for calculating the thermal resistance of a junction is based on Landauer theory and is given by[4]

$$R(\mathcal{L}_G) = \left[\frac{1}{(2\pi)^3} \sum_{\nu}^{+} \int_L c_{ph}(\boldsymbol{\kappa}, \nu, T) v_{g,z}(\boldsymbol{\kappa}, \nu) \alpha_{L\rightarrow R}(\boldsymbol{\kappa}, \nu, \mathcal{L}_G) d\boldsymbol{\kappa} \right]^{-1}. \quad (1)$$

The summation and integral are over all incident phonon modes in the first Brillouin zone of the left lead, $c_{ph}(\boldsymbol{\kappa}, \nu, T)$ is the mode-dependent phonon specific heat, which we evaluate at a temperature of 300 K using quantum (Bose-Einstein) statistics, and $v_{g,z}(\boldsymbol{\kappa}, \nu)$ is the z component of the group velocity vector (i.e., along the [001] direction).

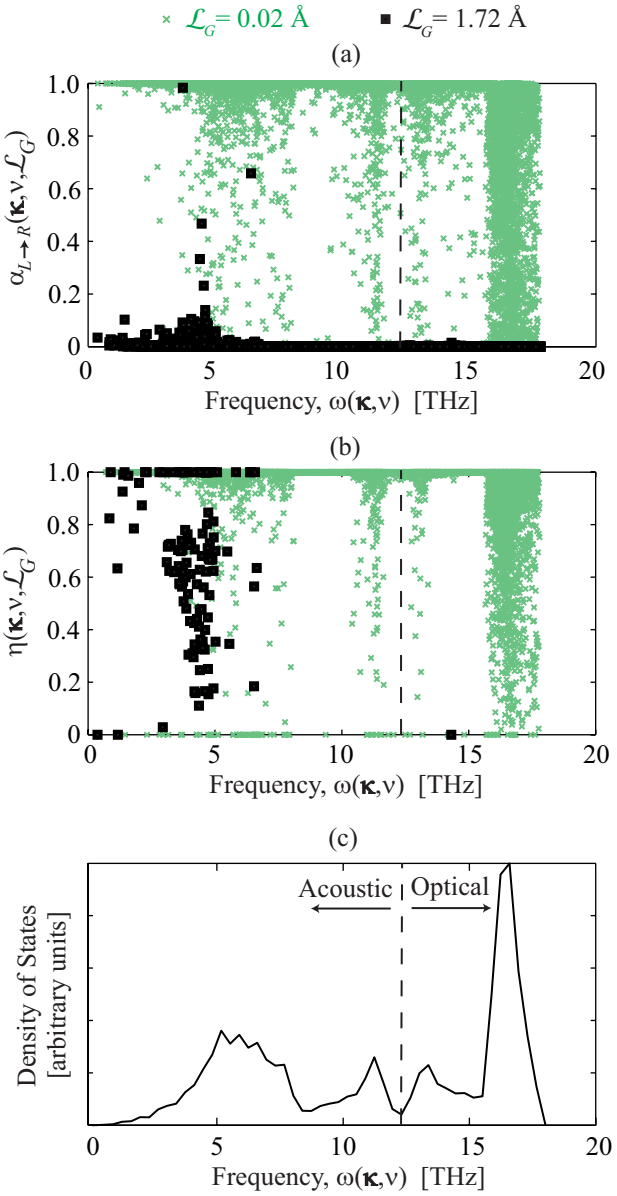

FIG. 2: (color online) Frequency dependence of (a) phonon transmission coefficient $[\alpha_{L\to R}(\boldsymbol{\kappa},\nu,\mathcal{L}_G)]$ for 10000 randomly sampled phonon modes in the first Brillouin zone and (b) the fraction of transmitted phonon energy that remains in its original eigenstate $[\eta(\boldsymbol{\kappa},\nu,\mathcal{L}_G)]$ for transmitted phonon modes with $\alpha_{L\to R}(\boldsymbol{\kappa},\nu,\mathcal{L}_G) > 0.01$. (c) Bulk phonon density of states for the silicon leads. The phonon density of states is calculated using a histogram with a bin width of 0.25 THz. The dashed line around 12 THz separates acoustic modes from optical modes.

It is well known that Eq. (1) incorrectly predicts a non-zero thermal resistance when applied to an ideal system with no interface (e.g., a perfect silicon crystal with no vacuum-gap, $\mathcal{L}_G = 0$).[4,19] To address this issue, Landry and McGaughey[14] combined the approaches of Simons[19] and Chen[20] to derive an expression for thermal resistance using

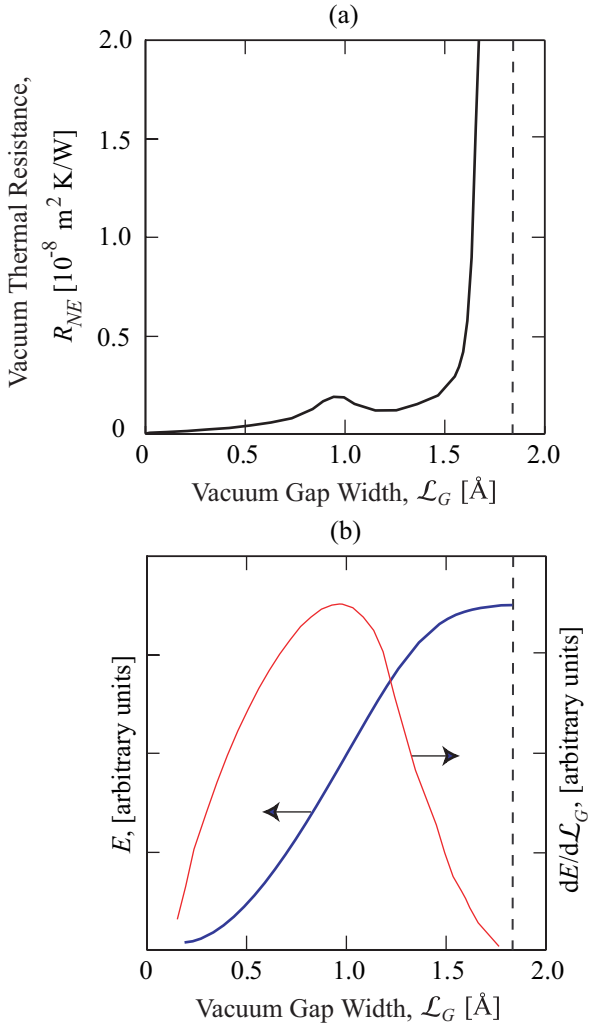

FIG. 3: (color online) (a) Vacuum thermal resistance (R_{NE}) as a function of vacuum-gap width ($\mathcal{L}_G$) at a temperature of 300 K. (b) Total lattice energy (E) and its derivative (dE/d$\mathcal{L}_G$) as a function of vacuum-gap width. The dashed line at $\mathcal{L}_G = 1.89$ $\mathring{A}$ corresponds to the Stillinger-Weber silicon potential cutoff ($\mathcal{L}_G^{cutoff}$).

the nonequilibrium (NE) phonon distributions in each lead, which they denote by R_{NE}:

$$R_{NE}(\mathcal{L}_G) = \left[1 - \frac{1}{(2\pi)^3}\sum_{\nu}^{+}\int_L \beta_L(\boldsymbol{\kappa},\nu,T)\alpha_{L\to R}(\boldsymbol{\kappa},\nu,\mathcal{L}_G)d\boldsymbol{\kappa} - \frac{1}{(2\pi)^3}\sum_{\nu}^{-}\int_R \beta_R(\boldsymbol{\kappa},\nu,T)\alpha_{R\to L}(\boldsymbol{\kappa},\nu,\mathcal{L}_G)d\boldsymbol{\kappa}\right] R(\mathcal{L}_G). \quad (2)$$

Here, $\beta_L(\boldsymbol{\kappa},\nu,T)$ and $\beta_R(\boldsymbol{\kappa},\nu,T)$ are the fraction of the total heat flux carried by a specific phonon mode in the leads.[14,20] We evaluate $\beta_L(\boldsymbol{\kappa},\nu,T)$ and $\beta_R(\boldsymbol{\kappa},\nu,T)$ at a temperature of 300 K using a model based on the Boltzmann transport equation under the relaxation-time approximation and the Fourier law.[14] Because bulk extents of silicon are considered on either side of the vacuum-gap, the bulk phonon properties that we previously predicted using harmonic and anharmonic lattice dynamics calculations[21,22] are used to evaluate Eqs. (1) and (2).

The lattice-dynamics predicted vacuum thermal resistances (R_{NE}) are plotted versus vacuum-gap width in Fig. 3(a). The limits of R_{NE} are intuitive. For a system with no vacuum-gap, the phonon transmission coefficient is one for all phonon modes. Under this condition, the two terms involving integrals in Eq. (2) are each equal to 1/2 and the vacuum thermal resistance is zero. As the vacuum-gap width increases and approaches $\mathcal{L}_G^{cutoff} = 1.89$ $\mathring{A}$ [the

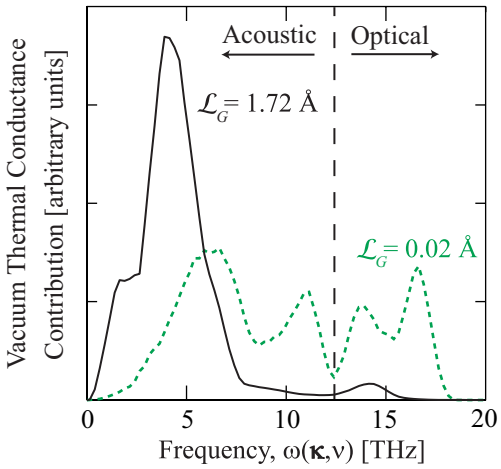

FIG. 4: (color online) Frequency-dependence of vacuum thermal conductance at a temperature of 300 K. The mode conductances are sorted using a histogram with a bin width of 0.25 THz. The dashed line around 12 THz separates acoustic modes from optical modes.

dashed line in Fig. 3(a)], the mode-dependent phonon transmission coefficients approach zero and the vacuum thermal resistance approaches infinity. We find no significant change to the phonon transmission coefficients or R_{NE} if the right silicon lead is shifted slightly (by 0.02 $\mathring{A}$) in the x or y direction such that the atomic monolayers in the right lead do not align with those in the left lead.

To understand the origin of the local maximum at $\mathcal{L}_G = 0.98$ $\mathring{A}$, the total lattice energy, E, and its derivative with respect to the vacuum-gap width, $\mathrm{d}E/\mathrm{d}\mathcal{L}_G$, are plotted as a function of $\mathcal{L}_G$ in Fig. 3(b). The local maximum in the vacuum thermal resistance coincides with the point of inflection of the total lattice energy, where $\mathrm{d}E/\mathrm{d}\mathcal{L}_G$ is maximum. Using electronic structure calculations on iron, Eberhart and MacLaren[23] showed that the second nearest neighbour bonds at the interface are broken at this point.

Although our calculations are performed using quantum statistics, there is no significant change to the vacuum thermal resistance results when classical (Maxwell-Boltzmann) statistics are used. This result is not surprising because quantum effects are not significant for Stillinger-Weber silicon at a temperature of 300 K (Ref. 22). In a classical harmonic calculation, $c_{ph}(\boldsymbol{\kappa}, \nu, T)$ is equal to k_B/V for all phonon modes,[9] where k_B and V are the Boltzmann constant and the volume of the left lead. We perform the following analysis in the classical limit to focus on the effects of $v_{g,z}(\boldsymbol{\kappa}, \nu)$ and $\alpha_{L\rightarrow R}(\boldsymbol{\kappa}, \nu, \mathcal{L}_G)$ on the mode-dependent contributions to the vacuum thermal conductance, which is the inverse of the vacuum thermal resistance.

The mode-dependent contributions to vacuum thermal conductance are plotted versus frequency for $\mathcal{L}_G = 0.02$ and 1.72 $\mathring{A}$ in Fig. 4.[18] In contrast to the typical assumption that optical phonons ($\omega > 12$ THz for Stillinger-Weber silicon) are negligible heat carriers in bulk because of their low group velocities [e.g., they contribute 3.5% to the bulk Stillinger-Weber silicon thermal conductivity at a temperature of 300 K (Ref. 21)], they contribute 32% to the vacuum thermal conductance for the $\mathcal{L}_G = 0.02$ $\mathring{A}$ structure. As noted in Section III, the phonon transmission coefficients strongly depend on phonon angle-of-incidence and are branch-independent for $\mathcal{L}_G = 0.02$ $\mathring{A}$. We thus attribute the large contributions of optical modes to their large phonon density of states [see Fig. 2(c)]. By including phonon dispersion in the DMM, Duda et al.[24] also found that the contribution of optical phonon modes to thermal boundary conductance can be significant. For $\mathcal{L}_G = 1.72$ $\mathring{A}$, only a few phonon modes contribute significantly to vacuum thermal conductance. Transverse acoustic modes are responsible for 90% of the transmitted phonon energy, with almost all of this contribution coming from phonon modes with $\kappa_z \mathcal{L}_G < 1$ (see discussion in Sec. III). Longitudinal acoustic (8.5%) and longitudinal optical (1.5%) modes make up the remaining 10%, while the contributions of transverse optical modes are negligible.

To put the results shown in Fig. 3(a) into perspective, we provide the phonon resistance of a Si/Si grain boundary[25] and a Si/Ge interface[14] predicted from molecular dynamics simulation using the Stillinger-Weber potential in Table I. The predicted resistances of both the Si/Si grain boundary and the Si/Ge interface are comparable to our lattice dynamics-based predictions for a 1 $\mathring{A}$ wide vacuum-gap. Although bulk vacuum is traditionally treated as a perfect phonon barrier, the results presented in Table I suggest that an angstrom-sized vacuum-gap should be treated as a phonon barrier with a finite resistance. One approach may be to treat the solid/vacuum-gap/solid structure as a system of two solids connected by weak springs. An example of this approach is described by Persson et al.[5]

Because vacuum phonon transport is a parallel heat-transfer process to near-field radiation, we now compare our

TABLE I: Vacuum thermal resistance predicted by lattice dynamics calculations and near-field radiation theory for a 1 $\mathring{A}$ wide vacuum-gap at a temperature of 300 K. Thermal boundary resistances for a Si/Si grain boundary and a Si/Ge interface predicted by molecular dynamics simulation using the Stillinger-Weber potential at a temperature of 500 K.

	Calculation Method	Resistance (m^2 K/W)
Si/vacuum-gap/Si (1 $\mathring{A}$ vacuum-gap)	Lattice Dynamics	0.19 x 10^{-8} (this work)
Si/vacuum-gap/Si (1 $\mathring{A}$ vacuum-gap)	Near-field Radiation Theory	0.12 x 10^{-4} (this work)
Si/Si Grain Boundary [Σ29(001)]	Molecular Dynamics	0.13 x 10^{-8} [25]
Si/Ge Interface	Molecular Dynamics	0.27 x 10^{-8} [14]

lattice dynamics-predicted phonon resistances to photon resistances predicted by near-field radiation theory. Classical radiation theory predicts that vacuum photon resistance is a constant. Near-field radiation theory, however, predicts that photon transport can be enhanced by the tunneling of evanescent waves and surface plasmon polaritons when vacuum-gap widths are sufficiently small (e.g., less than 10 microns wide for a Si/vacuum-gap/Si structure[27]). We calculate near-field radiative heat transfer in our Si/vacuum-gap/Si structures using Rytov's theory of fluctuational electrodynamics.[26–28] The resistance to photon energy transport and the resistance to phonon energy transport for a 1 $\mathring{A}$ wide vacuum-gap are provided in Table I. We find that the resistance to photon energy transport is four orders of magnitude larger than that to phonon energy transport.

Although vacuum phonon transport is not typically considered in AFM and STM studies, we have shown that atomic interactions between leads separated by a vacuum-gap can result in energy transport at a rate that is four orders of magnitude greater than predictions of near-field radiation theory. Altfeder et al.[1] experimentally observed a heat flux that was six orders of magnitude larger than predictions of near-field radiation theory. One explanation for this discrepency may be that the electric-field/lattice-deformation coupling mechanism proposed by Prunnila and Meltaus[2] is present in the STM tip-sample metal-metal junction studied by Altfeder et al.[1] but is not considered here. Because free electrons couple strongly to electric fields, the electron tunneling present in this STM experiment could have enhanced the atomic interactions between the leads. This hypothesis suggests directions for future study. First, how would phonon transport in a STM system be affected if the voltage difference that facilitates electron tunneling was removed? Second, can the effective range of vacuum phonon transport ($\mathcal{L}_G^{cutoff}$) be increased by taking advantage of electron tunneling?

V. SUMMARY

Although bulk vacuum is a classically impenetrable phonon barrier, we showed that phonons can transport across Angstrom-sized vacuum gaps due to atomic interactions between the leads. The thinner the vacuum-gap, the greater the energy transport [see Fig. 3(a)]. For a 1 $\mathring{A}$ wide vacuum-gap, the magnitude of phonon energy transport is comparable to that across a Si/Si grain boundary and four orders of magnitude greater than photon energy transport across the same structure (see Table I). While the vacuum-gaps studied in this work are atomically thin, they have important implications for thermal transport across macroscopic heterointerfaces where nanoasperities can play a crucial role in interface conductance.

Acknowledgments

We acknowledge financial support from the National Science and Engineering Research Council of Canada (DPS) and National Science Foundation grants DMR1006480 (AJHM) and CBET0853723 (KS and AN). We thank Jason M. Larkin (Carnegie Mellon University), Jonathan A. Malen (Carnegie Mellon University), and Charles A. Ward (University of Toronto) for helpful discussions.

[1] I. Altfeder, A. A. Voevodin, and A. K. Roy, Phys. Rev. Lett. **105**, 166101 (2010).
[2] M. Prunnila and J. Meltaus, Phys. Rev. Lett. **105**, 125501 (2010).
[3] G. D. Mahan, Applied Physics Letters **98**, 132106 (2011).
[4] E. T. Swartz and R. O. Pohl, Rev. Mod. Phys. **61**, 605 (1989).
[5] B. N. J. Persson, A. I. Volokitin, and H. Ueba, J. Phys.: Condense. Matter **23**, 045009 (2011).
[6] J.-H. Lee, J. C. Grossman, J. Reed, and G. Galli, Applied Physics Letters **91**, 223110 (2007).
[7] E. S. Landry and A. J. H. McGaughey, Journal of Applied Physics **107**, 013521 (2010).
[8] Z. T. Tian, B. E. White, Jr., and Y. Sun, Applied Physics Letters **96**, 263113 (2010).
[9] J. V. Goichochea, M. Marcela, and C. H. Amon, Journal of Heat Transfer **131**, 012401 (2009).
[10] F. H. Stillinger and T. A. Weber, Phys. Rev. B **31**, 5262 (1985).
[11] M. T. Dove, *Introduction to Lattice Dynamics* (Cambridge University Press, Cambridge, 1993).
[12] J. E. Turney, E. S. Landry, A. J. H. McGaughey, and C. H. Amon, Phys. Rev. B **79**, 064301 (2009).
[13] J. Wang and J. S. Wang, Phys. Rev. B **74**, 054303 (2006).
[14] E. S. Landry and A. J. H. McGaughey, Phys. Rev. B **80**, 165304 (2009).
[15] E. S. Landry, Ph.D. Thesis, Carnegie Mellon University, Pittsburgh, PA (2009).
[16] R. J. Stoner and H. J. Maris, Phys. Rev. B **48**, 16373 (1993).
[17] R. H. French, V. A. Parsegian, R. Podgornik, R. F. Rajter, A. Jagota, J. Luo, D. Asthagiri, M. K. Chaudhury, Y.-M. Chiang, S. Granick, et al., Rev. Mod. Phys. **82**, 1887 (2010).
[18] We first evaluate the square-bracketed term in Eq. (2) over the entire frequency domain. This term thus becomes a constant, mode-independent value. We then sort the mode-conductances using a histogram with a bin width of 0.25 THz.
[19] S. Simons, J. Phys. C: Solid State Phys. **7**, 4048 (1974).
[20] G. Chen, Applied Physics Letters **82**, 991 (2003).
[21] D. P. Sellan, J. E. Turney, A. J. H. McGaughey, and C. H. Amon, Journal of Applied Physics **108**, 113524 (2010).
[22] J. E. Turney, A. J. H. McGaughey, and C. H. Amon, Phys. Rev. B **79**, 224305 (2009).
[23] M. Eberhart and J. MacLaren, in *Innovations in Ultrahigh-Strength Steel Technology*, edited by G. B. Olson, M. Azrin, and E. S. Wright (1987), Sagamore Army Material Research Conference Proceedings: 34th, p. 693.
[24] J. C. Duda, T. E. Beechem, J. L. Smoyer, P. M. Norris, and P. E. Hopkins, Journal of Applied Physics **108**, 073515 (2010).
[25] S. Aubry, C. J. Kimmer, A. Skye, and P. K. Schelling, Phys. Rev. B **78**, 064112 (2008).
[26] S. M. Rytov, *Theory of Electric Fluctuations and Thermal Radiation* (Air Force Cambridge Research Center, Bedford, MA, 1959).
[27] A. I. Volokitin and B. N. J. Persson, Rev. Mod. Phys. **79**, 1291 (2007).
[28] A. Narayanaswamy and G. Chen, *Annual Review of Heat Transfer* (Begell House, 2005), pp. 169–195.